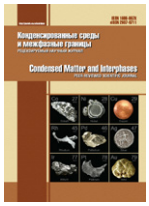

ISSN 1606-867X (Print)
ISSN 2687-0711 (Online)
Condensed Matter and Interphases
Kondensirovannye Sredy i Mezhfaznye Granitsy
https://journals.vsu.ru/kcmf/

Original articles

Research article
https://doi.org/10.17308/kcmf.2026.28/13554

Tunable magnetic, dielectric, and optical properties of cobalt ferrite/PVA nanocomposites: Effect of nanoparticle calcination temperature

Noor A. Saeed[1], Wafaa A. Hussain[1], Mukhlis M. Ismail[1], Mudatheer M. Al-Slivani[2]✉

[1]Department of Applied Physics, College of Applied Science, University of Technology, Baghdad, Iraq

[2]Al-Furqan University, College of Education for Pure Sciences, Department of Physics, Mosul, Iraq

Abstract

Objectives: This study investigates the magnetic and dielectric properties of nanocomposites composed of cobalt ferrite ($CoFe_2O_4$) nanoparticles embedded in a polyvinyl alcohol (PVA) matrix.

Experimental: $CoFe_2O_4$ nanoparticles were synthesized via a sol-gel auto-combustion method and subsequently calcined at 600 and 900 °C. X-ray diffraction results indicated that increasing the calcination temperature from 600 to 900 °C led to an increase in crystallite size from 23.3 nm to 48.5 nm. This was accompanied by an enhancement in saturation magnetization (*M*s) from 68.7 emu/g to 81.3 emu/g and a decrease in coercivity (*H*c) from 1150 to 860 Oe.

Conclusions: Most importantly, the PVA/$CoFe_2O_4$ composites exhibited enhanced dielectric properties compared to pure PVA. At 100 Hz, the dielectric constant (ε′) of the composite increased from approximately 18 (for PVA/CF600) to 42 (for PVA/CF900), values significantly higher than that of pure PVA, which was approximately 9. This enhancement highlights a synergistic effect between the ferrite nanoparticles and the polymer matrix, opening possibilities for designing composites with tunable dielectric responses for applications such as embedded capacitors and electromagnetic wave absorption devices.

Keyword: Cobalt ferrite, Nanocomposites, Polyvinyl alcohol (PVA), Magnetic properties, Dielectric constant, Optical band gap, Sol-gel

For citation: Saeed N. A., Hussain W. A., Ismail M. M., Al-Slivani M. M. Tunable magnetic, dielectric, and optical properties of cobalt ferrite/PVA nanocomposites: Effect of nanoparticle calcination temperature. *Condensed Matter and Interphases*. 2026;28(1): 3–14. https://doi.org/10.17308/kcmf.2026.28/13554

✉ Mudatheer M. Al-Slivani, e-mail: mudatheeralslivani@gmail.com

1. Introduction

Polymeric magnetic nanocomposites are of great scientific and technological interest since they can incorporate the inherent physical and chemical strength of organic polymers and gain the magnetic properties that are peculiar to nanoparticles [1–3]. These materials have benefits compared to traditional composites such as superior mechanical, thermal, and electrical characteristics and controllable magnetic action. Their versatility allows them to be used in a wide range of industries including water purification, medicine, dentistry, energy storage, environmental remediation, and delivering drugs [4–11]. Nanocomposites offer a promising field of study in the development of complex useful materials because particular design opportunities are offered through the incorporation of the magnetic nanoparticles in polymer matrices. Spinel ferrite nanocrystalline structures have received a lot of attention as they exhibit unique physical and chemical characteristics due to their surface effects and quantum confinement [12–17].

Cobalt ferrite ($CoFe_2O_4$) has been identified to be versatile and finds various uses including magnetic biosensing systems, drug delivery, and magnetic resonance imaging, alongside other magnetic ferrites. These nanoparticles can also be incorporated with polymers in nanocomposites with the magnetic particles being embedded in a non-magnetic matrix to make a soft ferrite system. This incorporation adds functional attributes to the material, and the material can be used in advanced biomedical and electronic gadgets [18]. The process of calcification of nanoparticles is effective in affecting the magnetic properties, particularly for those containing iron oxide, cobalt, nickel, and their compounds because of its explicit influence on the size and distribution of the nanoparticles by taking into account the changes that take place during the steps of nucleation and growth [19].

Magnetic characteristics are greatly affected by the size of the nanoparticles and changes in size distribution by modifying some of the parameters, including the coercivity (H_c), remanent magnetization (M_r), and saturation magnetization (M_s). Moreover, the surface and interface properties of the nanoparticles might be changed during the calcification process which in turn alters the magnetic behavior of the nanoparticles in addition to the above-mentioned processes; the surface oxidation, surface reconstruction, spin disorder, and magnetic coupling processes taking place on the surface of nanoparticles are all related to the calcification process, which is closely related them [20]. The calcification process is also accompanied by phase transitions and alterations in the crystalline structure of magnetic nanoparticles as is found with the phase transition of iron oxide maghemite or hematite into maghemite or hematite, respectively, in the presence of heat [21].

Nanoparticles grow in a directed manner during the calcification process resulting in different magnetic properties with the magnetic moments existing along the crystallographic directions. Conversely, conditioning creates defects and disturbances on the magnetic properties. E.g., lattice vacancies, dislocations, grain boundaries, which are created during the calcination process influence the magnetic field structure, the rotational process and the magnetic relaxation process of the magnetic nanoparticle. The calcification process influences the thermal stability and coercive strength and also promotes crystallization and granular development. The calcification process is regarded as an essential and significant action in enhancing the characterization of magnetic nanoparticles to be used in numerous applications like magnetic recording, magnetic sensors, and biomedical imaging among others because it is attained by enhancing the magnetic parameters [22–34].

PVA cobalt ferrite composites have already been prepared and investigated. As an example, Rashidi et al., 2016 [35] prepared the composite by mechanical alloying, which resulted in magnetic properties according to milling time. On the same note, Garcias-Cerda et al. (2007) [36] also made composite films and showed the reliance of their characteristics on the concentration of ferrite. The current work is characterized by the emphasis it placed on the pre-calcination temperature of the ferrite nanoparticles on the ultimate characteristics of the composite, a factor that has not been fully elaborated in the previous works. We show that the temperature of calcification can

be employed as an accurate means of modulating the dielectric constant of the composite.

This research is important as it provides valuable insights into how calcination temperature affects the magnetic and dielectric properties of cobalt ferrite nanoparticles embedded in a polyvinyl alcohol matrix. Understanding these effects is crucial for improving the performance of nanomaterials in a variety of applications, including sensors, magnetic storage, and biomedical devices. The study helps us to better understand how to optimize the properties of these nanocomposites, offering potential solutions for advanced technological and medical uses.

2. Experimental

Using an aqueous solution of cobalt nitrate and iron nitrate, with citric acid as a fuel, an ammonia solution was added until a pH of 7 was attained in the sol–gel auto combustion process. The mixture of metal nitrates and fuel (often in a molar ratio of 1:2:3). This mixture was heated to 80 °C on a magnetic stirrer while being continuously stirred to generate a viscous gel. After two hours of heating at 150 °C the gel undergoes self-propagating combustion that enabling the formation of ferrites. The resulting loose powder was thoroughly crushed and then calcined at 600 and 900 °C.

PVA granules (20 g) was added slowly to 100 ml of distilled room temperature water while stirring to prevent clumping. For complete dissolution, the solution put on a heated plate of magnetic stirrer at temperature 60 to 80 °C. The solution was held at this temperature for approximately five to seven hours to ensure full solubilization, by which point it turned transparent.

X-ray diffraction (XRD) was used to analyze the crystalline structure of the prepared powders using a Shimadzu XRD-6000 diffractometer with a voltage of 40 kV and a current of 30 mA, with Cu$K\alpha$ (1.5406 Å) radiation. The scan was carried out in the 2θ (20–80)° range. A JEOL JSM-6390LV Scanning Electron Microscope (SEM) was used to find out the morphology and the particle size. The Brunauer–Emmett–Teller (BET) method of surface area determination was used on a Quantachrome NOVA 2200e surface area analyzer to determine the specific surface area of the powders. Measurement of magnetic properties at room temperature was done with a Lake Shore 7404 Vibrating Sample Magnetometer (VSM). The dielectric characteristics of the PVA/$CoFe_2O_4$ composites were measured at a frequency of 100 Hz to 5 MHz on Agilent 4284A Precision LCR meter.

The experimental conditions were carefully selected based on established chemical principles and previous studies to ensure the synthesis of high-quality nanoparticles. The pH was adjusted to 7 to ensure the complete precipitation of metal ions and the formation of a homogeneous gel, which is optimal for the hydrolysis and condensation reactions in the sol-gel method. The 1:2:3 molar ratio of Co/Fe/fuel was chosen to provide a sufficient amount of fuel (citric acid) for a complete auto-combustion process, promoting the formation of the pure spinel phase while minimizing secondary phases. The calcination temperatures of 600 and 900 °C were selected to study the effect of the structural evolution from a nanocrystalline phase (at 600 °C) to a more well-defined crystalline structure (at 900°C) on the final properties of the nanocomposite.

A deliberate two-step methodology was employed to fundamentally understand the relationship between the nanoparticle filler and the final composite material. First, the standalone cobalt ferrite ($CoFe_2O_4$) powder was characterized (via XRD, SEM, BET) to establish its intrinsic properties (crystallite size, morphology, surface area) and their dependence on calcination temperature. These baseline properties are critical as they govern the subsequent behavior of the nanoparticles. Second, these well-characterized nanoparticles were embedded into the polyvinyl alcohol (PVA) matrix to investigate the composite's properties. The role of PVA is not passive but critical to the measurements. For the magnetic characterization (VSM), the PVA matrix acts as a separator, preventing nanoparticle agglomeration. This allows for the measurement of the magnetic response of largely isolated particles, thus providing a more accurate reflection of the size-dependent effects. For the optical measurements (UV-Vis), the measured band gap is a property of the composite system as a whole, arising from the electronic interactions between the ferrite filler and the polymer matrix.

Therefore, PVA is not merely a transparent medium but an active component that influences the final optical properties of the system.

3. Results and discussions

Fig. 1 shows the XRD results of the cobalt ferrite nanoparticles as-dried particles obtained at different temperatures (room temperature, 600, and 900 °C). XRD verified that the synthesized as-prepared and calcined $CoFe_2O_4$ were their crystal structure face-centered cubic (FCC) and phase identification with JCPDS card no. 22-1086 as shown in Fig. 1. The XRD analysis indicates that the result mostly indexed to $CoFe_2O_4$ with the miller indices of the reflection planes of (220), (311), (222), (400), (422), and (511). This pattern was also validated by previously studies [25, 26].

In comparison to the pure ferrite sample, the XRD peaks are wider, and this is correlated with the size of the nanocrystallite. As demonstrated in Fig. 1, calcination was carried out to eliminate secondary phases and remove internal stress that accompanying with the preparation of nanocobalt ferrite. When cobalt ferrite is calcined, the highest peak associated with the (311) plane which exhibits a higher diffraction angle increases with calcination as shown in Fig. 1. Also, Fig. 1 clearly illustrates shift of the highest peak (311) towards to higher 2θ angles, which suggests that there is a change in lattice constant with rising calcined temperature. When the calcined temperature reaches 600 °C, the peaks in the XRD pattern for $CoFe_2O_4$ become sharper, and their FWHM (full width at half maximum) decreases, indicating an increase in crystallite size. Based on the Williamson Hall (W-H) plot [27–29] (Fig. 2), the crystallite size and strain of the prepared $CoFe_2O_4$ are 44 nm and 0.00133 respectively. As seen in Fig. 2, it is observed that the crystallite size and strain also changes with the calcined temperature.

The crystallite size increased from 44 nm at room temperature to 56.68 and 73.1 nm at 600, and 900 °C as shown in Table 1. The growth of crystal size is attributed to the calcination process. This growth causes internal strains within the material. Due to differences in thermal expansion rates and grain boundaries, the characteristics of cobalt ferrite changed as the calcination temperature increased. The resulting lattice constants (*a*) of all powders are displayed in Table 1. It is evident that as the calcined temperature increased, the lattice constant increased. Thermal expansion of the crystal lattice resulted from increasing temperature, causing an increasing in the lattice constant. The X-ray density (ρ_x) results are illustrated in same Table. A slight decrease in X-ray density value is indicated with increasing temperatures. This result may be attributed to changes in crystal size

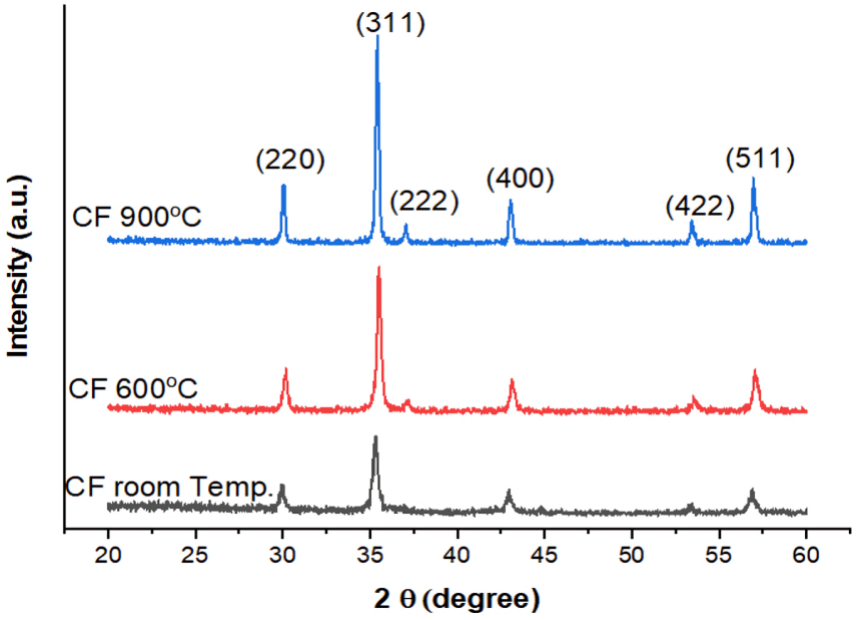

Fig. 1. XRD of CF (a) at room temperature, calcined at 600 and 900 °C

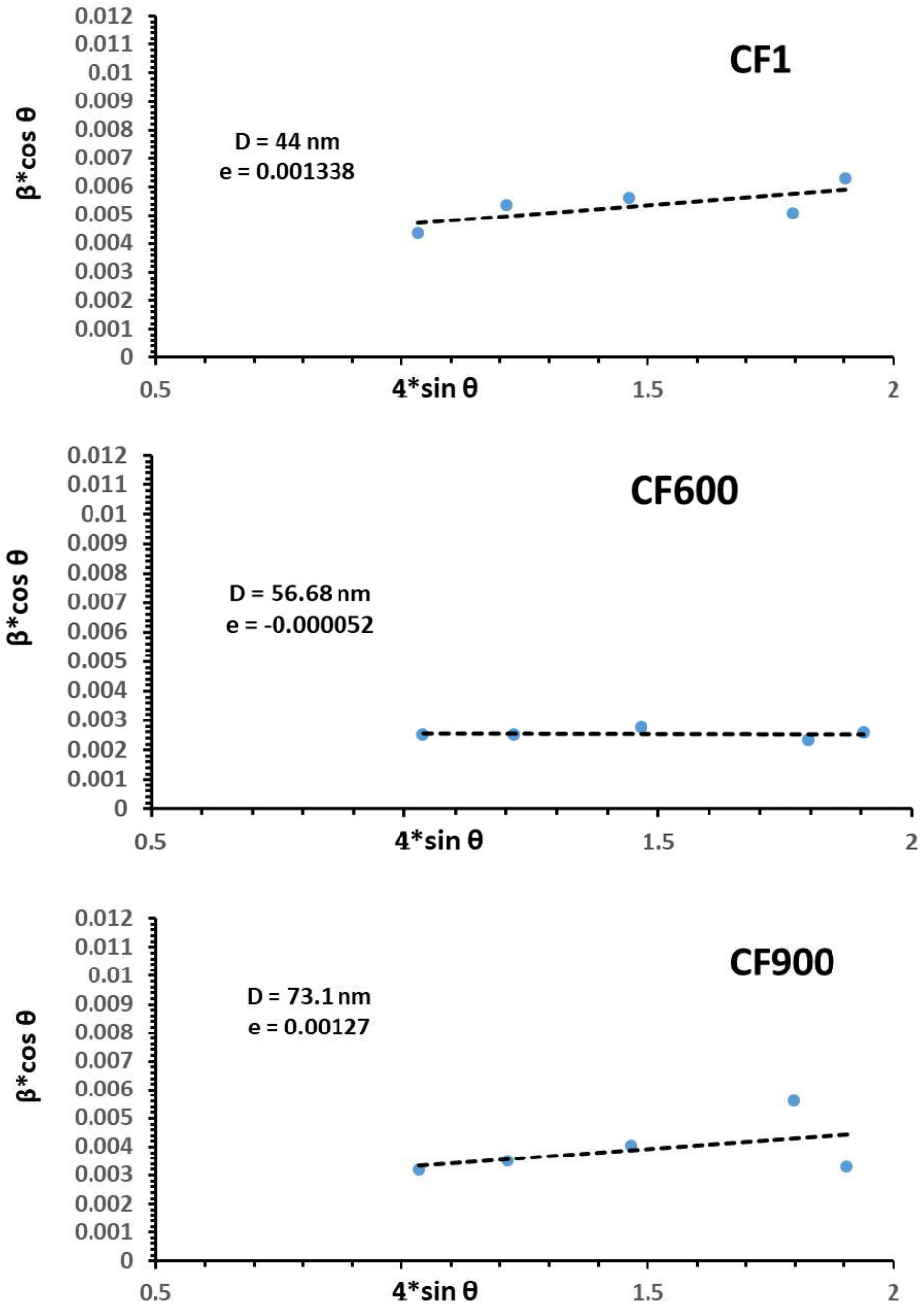

Fig. 2. W-H plot of CF at room temperature, calcined at 600 and 900 °C

and lattice parameters. Surface area per unit mass is called specific surface area (*S*) and its results are also listed in Table 1. The specific surface area values of room temperature and calcined powders have been reported to range between 26.1–15.6 (m^2/gm) as the calcined temperature increases.

This reduction is attributed to crystal size growth and particle agglomeration. In addition, the calculated values of hopping lengths for A-site (L_A) and B-site (L_B) are listed in Table (1). The hopping lengths of A-site and B-site are influenced by temperature. L_A and L_B were increased due to an expanding lattice parameter because of thermal expansion in which greater spacing between ions. The results of ionic radii (r_A) and (r_B) depending on oxygen positional parameter μ (= 0.0375 nm) and its radius of 0.135 nm are given in Table 1. Increasing

Table 1. Crystallite size *D*, strain, lattice constants (*a*), X-ray density (ρ_X), Specific area (*S*), the hopping lengths for A-site (L_A) and B-site (L_B), packing factor (*p*), and the tetrahedral (r_A) ionic radii and octahedral ionic radii (r_B)

Samples	CF1	CF600	CF900
Crystallite size *D* (nm)	44.001	56.681	73.123
Strain	0.001338	−0.00005	0.00127
Lattice constant *a* (Å)	8.374	8.404	8.420
X-ray density ρ_x (g/cm^3)	5.306	5.268	5.219
Specific area (*S*) (m^2/gm)	26.125	19.914	15.615
L_A (Å)	3.646	3.626	3.634
L_B (Å)	2.977	2.961	2.967
r_A (Å)	0.463	0.467	0.473
r_B (Å)	0.743	0.748	0.755
packing factor *(p)*	17.421	22.413	28.912

the calcination temperature of cobalt ferrite ($CoFe_2O_4$) leads to a larger ionic radius due to the expansion of the lattice. The packing factor (*P*) is a measure of how efficiently atoms are arranged in a crystal structure. The value of packing factor increases with higher calcination temperature due to enhanced crystallinity and particle growth as shown in Table 1. This growth leads to improve bulk density and higher packing factor, which is attributed to the heating of nanoparticles. The angle and the distance between atoms was determined with the help of the analysis using the HighScore Expert software. Also, the same program produced the Texture Coefficients and they were calculated using the following relationship provided in Equation [30, 31]:

$$d_{hkl} = 1/\sqrt{((h^2/a^2)+(k^2/b^2)+(l^2/c^2))}. \quad (1)$$

Where I_0 is the identified phase's XRD peak intensity, the peak intensities for all XRD are I_1, I_2, ... I_n.

FESEM images of CF nanoparticles annealed at various temperatures are displayed in Fig. 3. Images taken at room temperature showed that the fine particles were clumped together and had a spherical form. Due to the significant volume of gases released during combustion, pores or cavities were visible in the photographs of every sample. The porous network shown in Fig. 3 is a confirmed finding that is closely related to those powders prepared by combustion. As seen in Fig. 3, the nanoferrite particle size increased with the calcined temperature. At 900 °C, it is about 57.32 % (= 900/1570) of $CoFe_2O_4$ melting point (1570 °C), it is seen that the particle developed from separated single nanoparticles to compact nanoparticle granules. The micrometric aggregation shown in Fig. 3 can be explained by the occurrence of interaction between magnetic particles, especially at high temperatures, which could be primarily responsible for the occurrence of agglomerations [32–33]. Therefore, these nanoparticles exploit the thermal energy resulting from the calcination process to agglomerate, which results in the formation of larger granular particles. Fig. 4 displays the UV spectra of the PVA and PVA/CF composite. PVA's absorbance spectrum exhibits a distinctive peak at 200 nm that is related to the remaining acetate groups [34]. With a minor band position variation, the CF embedded PVA solutions exhibit every band seen in neat PVA and CF. As a result, the UV-vis spectra revealed relatively little absorbance in the visible wavelength range and primarily in the UV region. Using the Tauc plot as shown in Fig. 5, the energy gap for the PVA was found to be 3.87 eV, whereas it dropped to 3.1 eV for the PVA/CF composite where the cobalt nanoferrite was calcinated at 600 °C. As the degree of calcification of the ferrite increased, the energy gap began to increase, reaching 3.33 eV at 900 °C as shown in Fig. 6. Increasing the degree of calcination can cause significant changes in the crystal structure.

At low degrees of calcination, the degree of agglomeration in the nanoparticles is high, with crystallization being incomplete (as shown in Fig. 1 (XRD)), which leads to limiting the role and effectiveness of these nanoparticles. These obstacles can be overcome by increasing the degree of calcination, which in turn leads

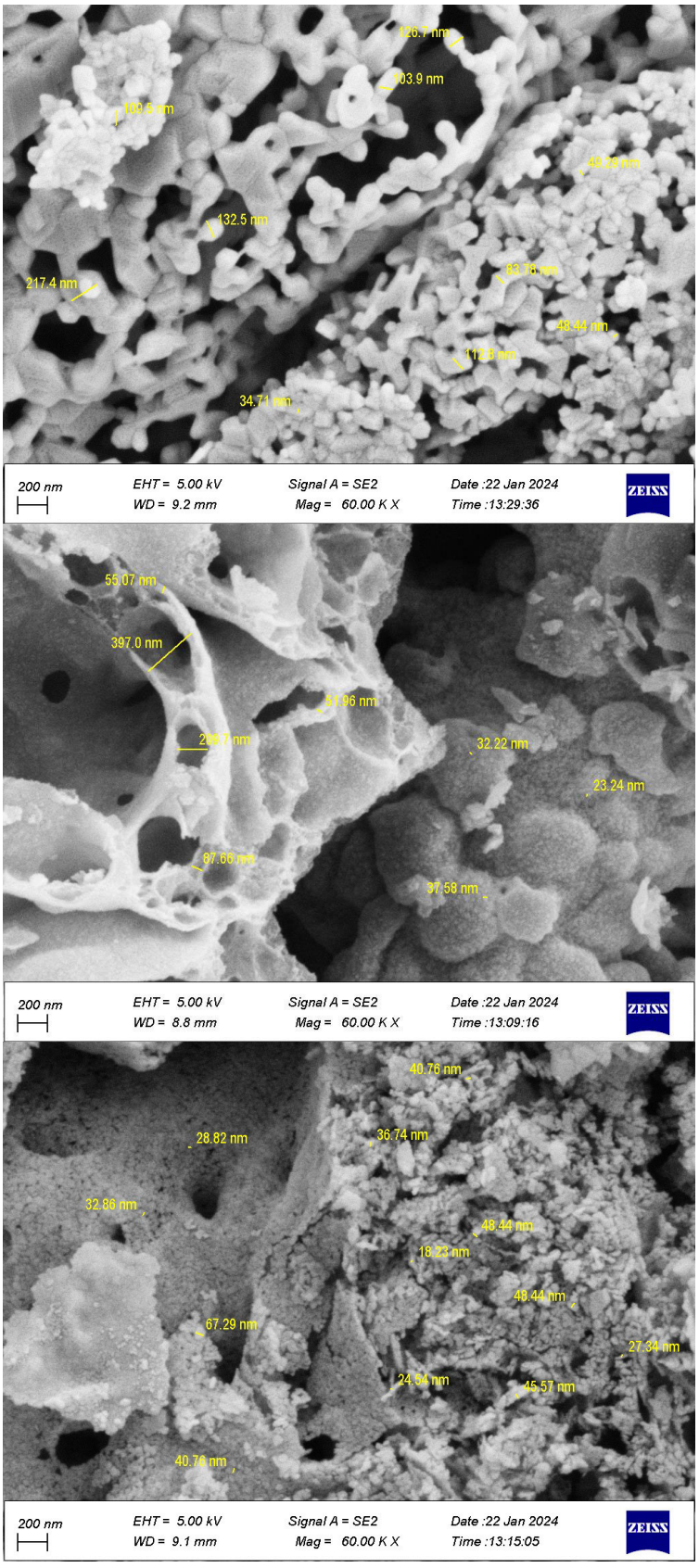

Fig. 3. Field Emission Scanning electron microscopy (FESEM) of CF at room temperature, calcined at 600 and 900 °C

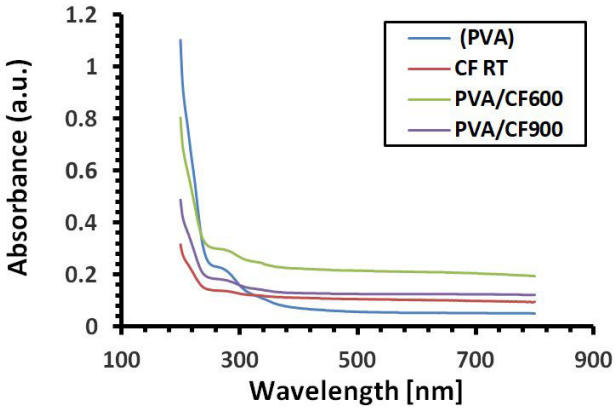

Fig. 4. UV-Vis spectra of PVA and PVA/CF composites

to an increase in the energy gap due to the phenomenon of quantum confinement. On the other hand, increasing calcination can affect the surface chemistry, as it leads to the removal of contaminants and surface defects such as oxygen vacancies, thus increasing the energy gap. Hysteresis loops (*M*-*H* curves) for PVA/CF composites are displayed in Fig. 6. The loops show saturation at 10000 Oe applied field. While the H_c values were noticeably high, the M_s and M_r values are low, most likely due to the influence of the small particle size. As the calcination temperature of cobalt ferrite increased, the saturation and

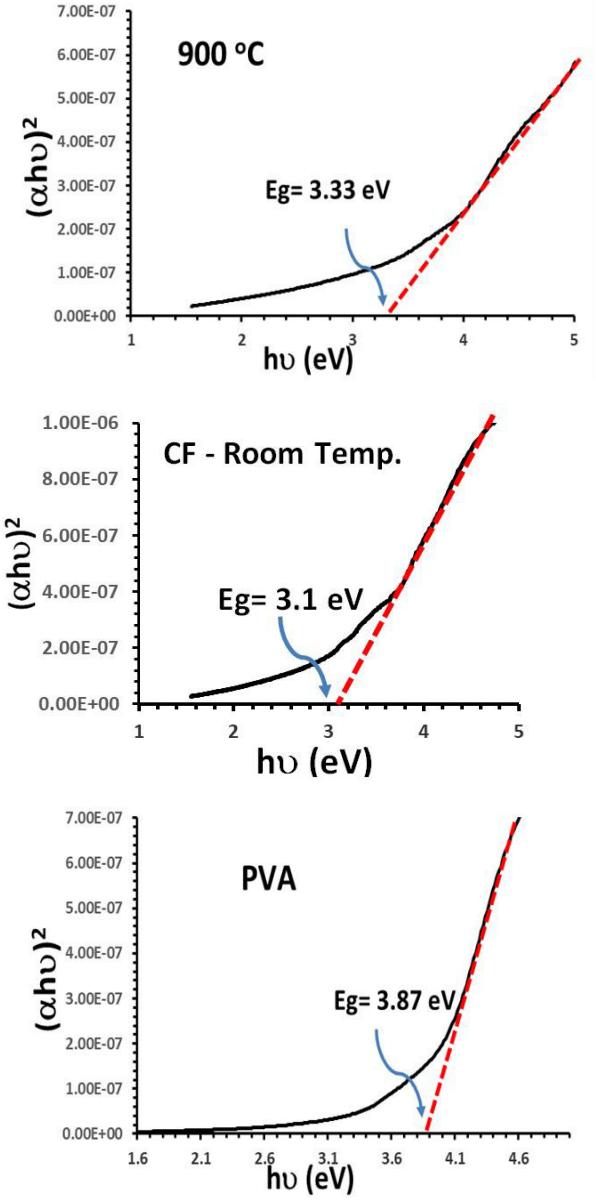

Fig. 5. Tauc plot of PVA and PVA/CF composites

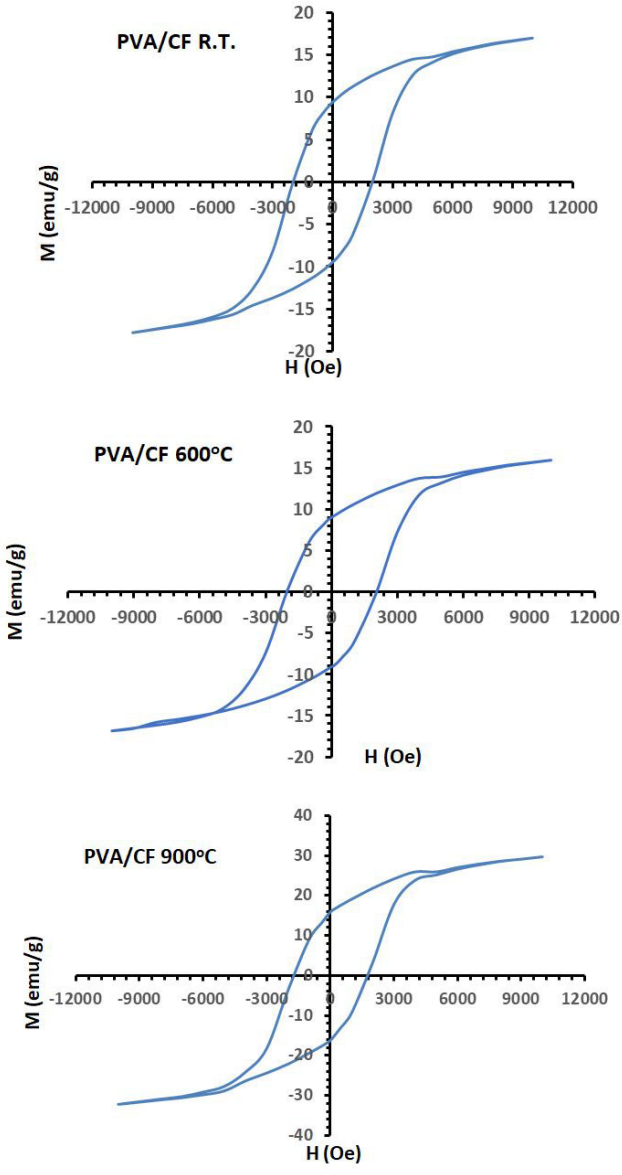

Fig. 6. *M*-*H* loop of PVA/CF composites

remnant magnetizations increased, while the coercivity decreased, as shown in Fig. 6. Calcination improves the crystallinity and intermolecular interaction of ferrites, where the crystallized materials mean a more efficient alignment of magnetic moments within the crystalline lattice, leading to higher magnetization. Also, calcination can reduce structural defects such as vacancies, dislocations, and grain boundaries in the CF that disrupt the alignment of magnetic moments.

The calcination of CF at high temperatures resulted in minimized defects. Together, these factors provide calcined ferrite materials with their improved magnetic characteristics and increased magnetization. The reduction of internal stresses, enhanced crystallinity, reduced structural defects, and composition optimization brought about by the calcination process are responsible for the overall decrease in coercivity seen with calcined CF. The effect of calcination temperature on the dielectric constant (ε) and dielectric loss of CF is shown in Fig. 7 and 8. The Fig. 7 shows the decrease of ε with increasing frequency and it increase with increasing degree of ferrite calcination. The Fig. 7 also shows that the dielectric constant of the PVA/CF600 composite appeared higher than that of the pure PVA, and its value increased more when the degree of calcination of the ferrite increased to 900 °C (PVA/CF900).

Table 2 summarizes the key magnetic parameters derived from the hysteresis loops for all samples. As indicated in the table, the saturation magnetization (M_s) exhibits a clear increase with rising calcination temperature, from 55.3 emu/g for the as-prepared sample (PVA/CFRT) to 81.3 emu/g for the sample treated at 900 °C (PVA/CF900). This enhancement is attributed to the improved crystallinity and growth of the nanoparticles. In contrast, the coercivity (H_c) decreases from 1350 to 860 Oe. This reduction is a typical behavior for ferrite nanoparticles as they grow larger and transition from a single-domain to a multi-domain magnetic structure.

The inhomogeneous microstructure and the superexchange connections are attributed to the dielectric behavior. The ascent and descent of the dielectric constant are significantly influenced by the grain boundaries. Furthermore, it was shown that the grain boundaries are more effective at lower frequencies. The grain effect in dielectric medium prevails at low frequency because the grain boundaries are low conductivity, while

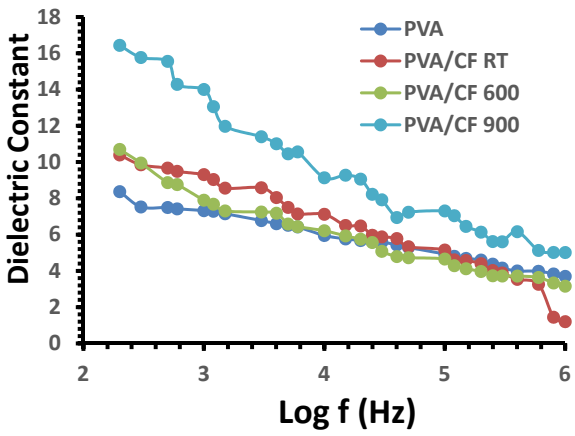

Fig. 7. Dielectric constant of PVA and PVA/CF composites

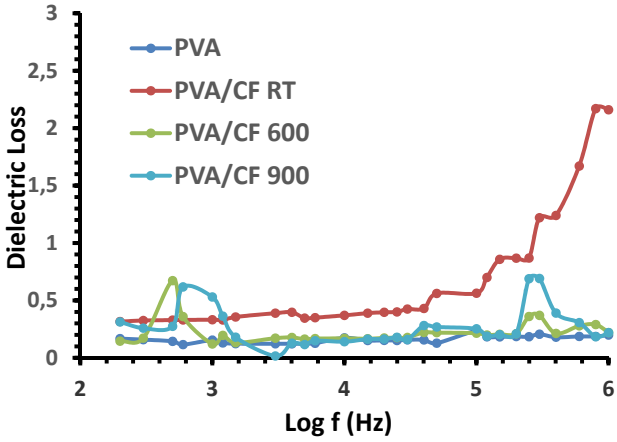

Fig. 8. Dielectric constant of PVA and PVA/CF composites

Table 2. Magnetic parameters of the PVA/$CoFe_2O_4$ nanocomposite samples

Sample	Saturation Magnetization (M_s) (emu/g)	Coercivity (H_c) (Oe)	Remanence (M_r) (emu/g)
PVA/CFRT	55.3	1350	23.4
PVA/CF600	68.7	1150	28.5
PVA/CF900	81.3	860	22.1

the grains are conductive. Because of the charge carriers, polarization becomes much slower in the high-frequency region when an AC field is applied. The reason for this result is that the particle suffers changes from separated single particles to compact nanoparticle granules. As frequency increases, dielectric loss decreases as seen in Fig. 8, where the interface that separates conductive from insulating nature plays a significant role. This is shown by the fact that PVA/CF nanocomposites exhibit a higher dielectric loss than the PVA, which could be attributed to the micro-mechanical stress, and effect of surface depolarization domain wall. The low conductivity and dielectric loss in pure PVA is due to the amorphous nature of the surface, which can be avoided by charge transfer from the ligand to the metal added in the PVA chain, which leads to increased packing density and probabilistic, which supports dielectric behavior.

The observed increase in the dielectric constant of the composite with higher ferrite calcination temperature is a highly desirable property for numerous technological applications. Materials with a high dielectric constant are required for the fabrication of embedded capacitors in electronic devices, as they allow for storing more energy in a smaller volume. They also play a critical role in microwave absorption and electromagnetic interference (EMI) shielding applications, where the material's ability to store electrical energy contributes to the dissipation of unwanted electromagnetic wave energy. The ability to tune the band gap of the composite opens doors for applications in optoelectronics. For instance, a material with a tunable band gap could be used in photosensors or in photocatalysis, where the band gap value determines the wavelength of light the material can efficiently absorb and interact with. The increase in the band gap we observed could enhance the material's stability under high electric fields and reduce leakage currents in electronic devices.

4. Conclusion

The investigation into the magnetic and dielectric properties of cobalt ferrite ($CoFe_2O_4$) nanoparticles embedded in a polyvinyl alcohol (PVA) matrix under varying calcination temperatures has demonstrated the significant influence of thermal treatment on the material's properties. The study showed that increasing calcination temperature from room temperature to 900 °C enhances the crystallinity and magnetic characteristics of the nanocomposite. The crystallite size increased, and structural defects were minimized, leading to improved magnetization and reduced coercivity. Notably, the dielectric constant and loss also exhibited a temperature-dependent enhancement, with higher calcination temperatures contributing to superior material performance. These findings underline the critical role of the calcination process in optimizing the magnetic and dielectric behavior of PVA/$CoFe_2O_4$ composites for potential applications in areas such as energy storage, biomedical imaging, and magnetic sensors. Furthermore, the study highlights the synergistic effect between the polymer matrix and magnetic nanoparticles, offering an insight into the design of advanced nanocomposites with tunable properties. Thus, the research opens avenues for further exploration into the tailoring of magnetic and dielectric properties in nanocomposite systems for specialized applications.

Author contributions

Noor A. Saeed and Mudatheer M. Al-Slivani conceived the study and designed the experiments. Wafaa A. Hussain performed the synthesis and characterization. Mukhlis M. Ismail analyzed the data. All authors wrote and reviewed the manuscript.

References

1. Romero-Fierro D., Bustamante-Torres M., Bravo-Plascencia F., Magaña H., Bucio E. Polymer-magnetic semiconductor nanocomposites for industrial electronic applications. *Polymers*. 2022;14(12): 2467. https://doi.org/10.3390/polym14122467

2. Shivamurthy S., Yashas R., Shahmoradi B., Wantala K., Shivaraju H. P. Potentiality of polymer nanocomposites for sustainable environmental applications: a review of recent advances. *Polymer*. 2021;233: 124184. https://doi.org/10.1016/j.polymer.2021.124184

3. Popova V., Dmitrienko E., Chubarov A. Magnetic nanocomposites and imprinted polymers for biomedical applications of nucleic acids. *Magnetochemistry*. 2023;9(1): 12. https://doi.org/10.3390/magnetochemistry9010012

4. Ziedan W., Hussain W. A., Ismail M. M. Porous adsorbent based on kaolin and nanomagnetic cobalt ferrite for effective removal of Pb(II) from wastewater. *Journal of Superconductivity and Novel Magnetism*. 2024;37: 587–596. https://doi.org/10.1007/s10948-024-06700-1

5. Hussain W. A., Al-Mosawe E. H. A., Ismail M. M., Alwan L. H. Porous biphasic calcium phosphate for biomedical application. *Journal of Biomimetics, Biomaterials and Biomedical Engineering*. 2021;49: 101–110. https://doi.org/10.4028/www.scientific.net/jbbbe.49.101

6. Hashim F. S., Ismail M. M., Hussain W. A. Tri-calcium phosphate (nanoparticles/nanofibers)/PVA for bone tissue engineering. *Acta Physica Polonica A*. 2021;140(4): 337–343. https://doi.org/10.12693/aphyspola.140.337

7. Assim F., Al-Mosawe E. H. A., Hussain W. A. Studying the physical and biological characteristics of denture base resin PMMA reinforced with ZrO_2 and TiO_2 nanoparticles. *Karbala International Journal of Modern Science*. 2022;8(4): 503–513. https://doi.org/10.33640/2405-609x.3268

8. Ismail M. M., Hussain W. A., Hashim F. S. Bio-application of poly (vinyl alcohol)/biphasic calcium phosphate scaffold as bone tissue replacement. *Current Materials Science*. 2022;15(3): 271–279. https://doi.org/10.2174/2666145415666220330110601

9. Taher S. Y., Hussain W. A. The effect of acidic treatment of carbon fiber on denture mechanical properties. *Journal of Physics: Conference Series*. 2021;1879(3): 032082. https://doi.org/10.1088/1742-6596/1879/3/032082

10. Hussain W. A., Ismail M. M., Taher S. Incorporation of treated woven carbon fiber to methacrylate resin for heat-cured acrylic denture composite. *Journal of Biomimetics, Biomaterials and Biomedical Engineering*. 2022;56: 153–164. https://doi.org/10.4028/p-627g18

11. Hussain W. A., Jawad S. M. H. A., Hannon S. A Effect of carbon fibre layer with alumina and tri calcium phosphate on mechanical properties of denture base. *International Journal of Nano and Biomaterials*. 2021;10(1): 22–33. https://doi.org/10.1504/ijnbm.2021.114691

12. Saha M., Mukherjee S., Bera P., Seikh Md. M., Gayen A. Structural, optical, dielectric, and magnetic properties of spinel MFe_2O_4 (M = Co and Zn) nanoparticles synthesized by CTAB-assisted hydrothermal method. Ceramics *International*. 2022;48(23): 35719–35732. https://doi.org/10.1016/j.ceramint.2022.07.058

13. Salih S. J., Mahmood W. M. Review on magnetic spinel ferrite (MFe_2O_4) nanoparticles: from synthesis to application. *Heliyon*. 2023;9(12): e16601. https://doi.org/10.1016/j.heliyon.2023.e16601

14. Ravinder D., Hashim M., Upadhyay A., … Khalilullah A. Structural, elastic and magnetic properties of Co-Mg nanoferrites. *Solid State Communications*. 2022;342: 114629. https://doi.org/10.1016/j.ssc.2021.114629

15. Ismail M. M., Jaber N. A. Structural analysis and magnetic properties of lithium-doped Ni-Zn ferrite nanoparticles. *Journal of Superconductivity and Novel Magnetism*. 2018;31(6): 1917–1923. https://doi.org/10.1007/s10948-017-4428-3

16. Ismail M. M., Jaber N. A. Structural and elastic properties of nickel–zinc ferrite nano-particles doped with lithium. *Journal of the Brazilian Society of Mechanical Sciences and Engineering*. 2018:40(5): 250. https://doi.org/10.1007/s40430-018-1164-y

17. Rafeeq S. N., Ismail M. M., Sulaiman J. M. A. (2017). Magnetic and dielectric properties of $CoFe_2O_4$ and $Co_xZn_{1-x}Fe_2O_4$ nanoparticles synthesized using sol-gel method. *Journal of Magnetics*. 2017;22(3): 406–413. https://doi.org/10.4283/jmag.2017.22.3.406

18. Farzaneh S., Hosseinzadeh S., Samanipour R., Hatamie S., Ranjbari J., Khojasteh A. Fabrication and characterization of cobalt ferrite magnetic hydrogel combined with static magnetic field as a potential bio-composite for bone tissue engineering. *Journal of Drug Delivery Science and Technology*. 2021;64: 102525. https://doi.org/10.1016/j.jddst.2021.102525

19. Basak M., Rahman Md. L., Ahmed Md. F., Biswas B., Sharmin N. Calcination effect on structural, morphological and magnetic properties of nano-sized $CoFe_2O_4$ developed by a simple co-precipitation technique. *Materials Chemistry and Physics*. 2021;264: 124442. https://doi.org/10.1016/j.matchemphys.2021.124442

20. Mahdi S. H., Jassim W. H., Hamad I. A., Jasima K. A. Epoxy/silicone rubber blends for voltage insulators and capacitors applications. *Energy Procedia*. 2017;119: 501–506. https://doi.org/10.1016/j.egypro.2017.07.059

21. Aleabi S. H., Watan A. W., Salman E. M.-T., Jasim K. A., Shaban A. H., AlSaadi T. M. The study effect of weight fraction on thermal and electrical conductivity for unsaturated polyester composite alone and hybrid. *AIP Conference Proceedings*. 2018;1968(1): 020019. https://doi.org/10.1063/1.5039178

22. Hu P., Chang T., Chen W.-J., … Volinsky A. A. Temperature effects on magnetic properties of Fe_3O_4 nanoparticles synthesized by the sol-gel explosion-assisted method. *Journal of Alloys and Compounds*. 2019;773: 605–611. https://doi.org/10.1016/j.jallcom.2018.09.238

23. Purnama B., Wijayanta A. T., Suharyana. Effect of calcination temperature on structural and magnetic properties in cobalt ferrite nano particles. *Journal of King Saud University – Science*. 2019;31(4): 956–960. https://doi.org/10.1016/j.jksus.2018.07.019

24. Akbarzadeh A., Samiei M., Davaran S. Magnetic nanoparticles: preparation, physical properties, and applications in biomedicine. *Nanoscale Research Letters*. 2012;7(1): 144. https://doi.org/10.1186/1556-276x-7-144

25. Hashim M., Ahmed A., Ali S. A., … Ravinder D. Structural, optical, elastic and magnetic properties of Ce and Dy doped cobalt ferrites. *Journal of Alloys and Compounds*. 2020;834: 155089. https://doi.org/10.1016/j.jallcom.2020.155089

26. Hashim M., Boda N., Ahmed A., … Nasir M. Influence of samarium doping on structural, elastic, magnetic, dielectric, and electrical properties of nanocrystalline cobalt ferrite. *Applied Physics A*. 2021;127(7): 526. https://doi.org/10.1007/s00339-021-04686-4

27. Ismail M. M., Jaber N. A. Effect of Li doping on the microstructure and some physical properties of Ni-Zn ferrite nanoparticles. *Surface Review and Letters*. 2018;25(03): 1850076. https://doi.org/10.1142/s0218625x18500762

28. Salman O. N., Agool I. R., Ismail M. M. Preparation of the scattering layer based on TiO_2 nanotube and their dye sensitized solar cell applications. *Applied Physics A*. 2017;123(6). https://doi.org/10.1007/s00339-017-1012-4

29. Ismail M. M., Shaker S. S., Kamil R. A. Influence of pulse laser energy on structural and magnetic properties of $CoFe_2O_4$ and $CoLa_{0.01}Fe_{1.99}O_4$ thin films. *ECS Journal of Solid State Science and Technology*. 2023;12(3): 033005. https://doi.org/10.1149/2162-8777/acc136

30. Al-Slivani M. M., Hammod M. A., Abed M. A. Partial substitution effect of silver on the structural and electrical

properties of high temperature superconductor ($Bi_{2-x}Ag$–$Ba_2Ca_2Cu_3O_{10+\delta}$). *Ochrona Przed Korozja*. 2025;68(1): 15–20. https://doi.org/10.15199/40.2025.3.2

31. Al-Slivani M. M., Hammod M. A., Abed M. A. Double partial substitution effect of silver (Ag) and strontium (Sr) on the structural and electrical properties of high temperature $Bi_{2-x}Ag_xBa_{2-y}Sr_yCa_2Cu_3O_{10+\delta}$ superconductor. *Functional Materials*. 2025;32(1): 42–49. https://doi.org/10.15407/fm32.01.42

32. Priyadharsini P., Pradeep A., Chandrasekaran G. Novel combustion route of synthesis and characterization of nanocrystalline mixed ferrites of Ni–Zn. *Journal of Magnetism and Magnetic Materials*. 2009;321(12): 1898–1903. https://doi.org/10.1016/j.jmmm.2008.12.005

33. To Loan N. T., Hien Lan N. T., Thuy Hang N. T., ... Van Tran T. $CoFe_2O_4$ nanomaterials: effect of annealing temperature on characterization, magnetic, photocatalytic, and photo-fenton properties. *Processes*. 2019;7(12): 885. https://doi.org/10.3390/pr7120885

34. Guirguis O. W., Moselhey M. T. H. Optical study of poly(vinyl alcohol)/hydroxypropyl methylcellulose blends. *Journal of Materials Science*. 2011;46(17): 5775–5789. https://doi.org/10.1007/s10853-011-5533-5

35. Rashidi S., Ataie A. Structural and magnetic characteristics of PVA/$CoFe_2O_4$ nano-composites prepared via mechanical alloying method. *Materials Research Bulletin*. 2016;80: 321–328. https://doi.org/10.1016/j.materresbull.2016.04.021

36. García-Cerda L. A., Escareño-Castro M. U., Salazar-Zertuche M. Preparation and characterization of polyvinyl alcohol–cobalt ferrite nanocomposites. *Journal of Non-Crystalline Solids*. 2007;353(8–10): 808–810. https://doi.org/10.1016/j.jnoncrysol.2006.12.046

Information about the authors

Noor A. Saeed, M.Sc., Assistant Lecturer, Researcher, Department of Applied Physics, College of Applied Science, University of Technology (Baghdad, Iraq).
https://orcid.org/0009-0001-0488-7230
as.22.57@grad.uotechnology.edu.iq

Wafaa A. Hussain, PhD, Professor, Department of Applied Physics, College of Applied Science, University of Technology (Baghdad, Iraq).
https://orcid.org/0000-0002-0994-9381
100067@uotechnology.edu.iq

Mukhlis M. Ismail, PhD, Professor, Department of Applied Physics, College of Applied Science, University of Technology (Baghdad, Iraq).
https://orcid.org/0000-0002-7834-4191
mmismail009@gmail.com

Mudatheer M. Al-Slivani, M.Sc., Assistant Lecturer, Department of Physics, College of Education for Pure Sciences, Al-Furqan University (Mosul, Iraq).
https://orcid.org/0009-0004-5231-7461
mudatheeralslivani@gmail.com

Received September 2, 2025; approved after reviewing December 4, 2025; accepted for publication January 15, 2026; published online April 01, 2026.